Redox Biology 24 (2019) 101183

Contents lists available at ScienceDirect

Redox Biology

journal homepage: www.elsevier.com/locate/redox

Research Paper

The early response of αB-crystallin to a single bout of aerobic exercise in mouse skeletal muscles depends upon fiber oxidative features

Ivan Dimauro[a,*], Ambra Antonioni[a], Neri Mercatelli[a], Elisa Grazioli[a], Cristina Fantini[a], Rosario Barone[b,c], Filippo Macaluso[b,c,d], Valentina Di Felice[b], Daniela Caporossi[a]

[a] Unit of Biology and Genetics, Department of Movement, Human and Health Sciences, University of Rome "Foro Italico", Piazza Lauro de Bosis 15, 00135, Rome, Italy
[b] Department of Biomedicine, Neuroscience and Advanced Diagnostics (BiND), Section of Human Anatomy, University of Palermo, Palermo, Italy
[c] Euro-Mediterranean Institutes of Science and Technology (IEMEST), Palermo, Italy
[d] SMART Engineering Solutions & Technologies (SMARTEST) Research Center eCampus University, Novedrate, CO, Italy

ARTICLE INFO

Keywords:
αB-crystallin phosphorylation
Endurance exercise
Oxidative stress
Skeletal muscle

ABSTRACT

Besides its substantial role in eye lens, αB-crystallin (HSPB5) retains fundamental function in striated muscle during physiological or pathological modifications. In this study, we aimed to analyse the cellular and molecular factors driving the functional response of HSPB5 protein in different muscles from mice subjected to an acute bout of non-damaging endurance exercise or in C2C12 myocytes upon exposure to pro-oxidant environment, chosen as "*in vivo*" and "*in vitro*" models of a physiological stressing conditions, respectively.

To this end, red (GR) and white *gastrocnemius* (GW), as sources of slow-oxidative and fast-glycolytic/oxidative fibers, as well as the *soleus* (SOL), mainly composed of slow-oxidative type fibers, were obtained from BALB/c mice, before (CTRL) and at different times (0′, 15′, 30′ 120′) following 1-h of running. Although the total level of HSPB5 protein was not affected by exercise, we found a significantly increase of phosphorylated HSPB5 (*p*-HSPB5) only in GR and SOL skeletal muscle with a higher amount of type I and IIA/X myofibers. The fiber-specific activation of HSPB5 was correlated to its interaction with the actin filaments, as well as to an increased level of lipid peroxidation and carbonylated proteins. The role of the pro-oxidant environment in HSPB5 response was investigated in terminally differentiated C2C12 myotubes, where most of HSPB5/pHSPB5 pool was present in the cytosolic compartment in standard culture conditions. As a result of exposure to pro-oxidizing, but not cytotoxic, H_2O_2 concentration, the p-38MAPK-mediated phosphorylation of HSPB5 resulted functional to promote its interaction with the myofibrillar components, such as β-actin, desmin and filamin 1.

This study provides novel information on the molecular pathway underlying the HSPB5 physiological function in skeletal muscle, confirming the contribution of the pro-oxidant environment in HSPB5 activation and interaction with substrate/client myofibrillar proteins, offering new insights for the study of myofibrillar myopathies and cardiomyopathies.

1. Introduction

In mammals, the family of small Heat Shock Proteins (sHSPs) represents a class of ATP-independent chaperones able to trap misfolded proteins through a so-called "holdase" activity and therefore avoiding their aggregation [1]. sHSPs family displays different functions depending on tissue, intracellular localization, developmental expression as well as the level of the induction and protein targets. Among sHSPs, the most prominent and well-studied member of the family is αB-crystallin (HSPB5), a protein playing a critical role in the modulation of several cellular processes related to survival and stress recovery, such as protein degradation, cytoskeletal stabilization, and apoptosis [2,3].

In the past, numerous studies have shown the important function of this protein in striated muscle during physiological or pathological changes [4–11]. In adult mammalian skeletal muscle, HSPB5 is constitutively expressed, with higher levels in the slow-twitch fibers than in the fast-twitch ones [12]. Experimental data suggest that this sHSP protects mammalian skeletal muscle from heat, oxidative stress, and mechanical stresses produced during middle age and senescence or by physical activity [5,13–18], and its role in maintaining musculoskeletal

* Corresponding author.
E-mail addresses: ivan.dimauro@uniroma4.it (I. Dimauro), ambra.anto@hotmail.it (A. Antonioni), mastroneri@hotmail.com (N. Mercatelli), elisalillygrazioli@gmail.com (E. Grazioli), cristina.fantini@uniroma4.it (C. Fantini), rusbarone@hotmail.it (R. Barone), fil.macaluso@gmail.com (F. Macaluso), valentina.difelice@unipa.it (V. Di Felice), daniela.caporossi@uniroma4.it (D. Caporossi).

https://doi.org/10.1016/j.redox.2019.101183
Received 20 February 2019; Received in revised form 21 March 2019; Accepted 28 March 2019
Available online 03 April 2019

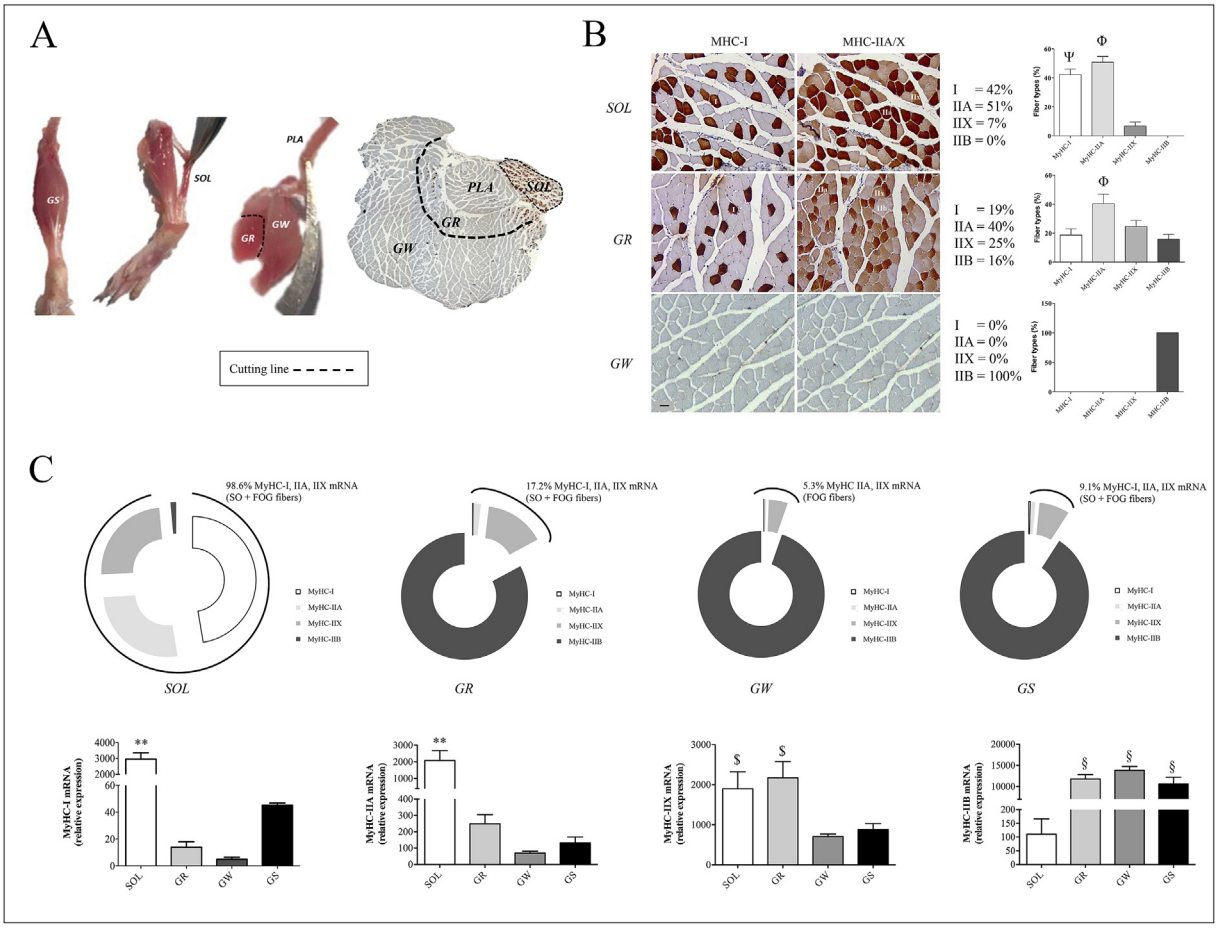

Fig. 1. Analysis of the muscle type fibers in the posterior group of hindlimb muscles (i.e. *Soleus*, *Gastrocnemius* Red and White). (**A**) Images of mouse hindlimb muscles and a cross-section showing the cuts made during the dissection of the muscles. (**B**) Representative images used for quantitative analysis of serial cross-sections immunostained for MHC-I and MHC-IIA/X. Type IIB fibers are negative to antibodies anti-MHC-I and anti-MHC-IIA/X. The analysis was performed using 5 fields per section, 5 sections per mice (40 μm) between sections). An average of 400 fibers was analysed for each mouse. The percentage of the fibers was shown as histogram. (**C**) qRT-PCR analysis of MyHC genes levels. The exploded doughnut shows the percentage of MyHC isoforms expression in SOL, GR, GW and GS. Bar of each histogram shows the MyHC isoforms gene expression levels normalized for the reference gene ($2^{-\Delta CT}$). Intermediate hybrid fibers were not taken into consideration in these analyses because of their limited number. Data are presented as means ± SD. Statistical significance was determined using a one-way ANOVA with Bonferroni's post-hoc test. Φ $p < 0.01$ *vs.* all MyHC isoforms; Ψ $p < 0.01$ *vs.* MHC-IIX and MHC-IIB; **$p < 0.01$ *vs.* all other tissues; $ $p < 0.05$ *vs.* GW and GS; §$p < 0.01$ *vs.* SOL. **SO**, Slow Oxidative fibers; **FOG**, Fast Oxidative-Glycolytic fibers; **GR**, Gastrocnemius red; **GW**, Gastrocnemius white; **SOL**, Soleus; **GS**, Whole Gastrocnemius.

functions is highlighted in a number of known disorders where *HspB5* gene is mutated or overexpressed [19].

It is widely accepted that, depending upon type, intensity, frequency and duration, exercise leads to modulation of activity and/or expression of sHSPs, including HSPB5, in mammalian skeletal muscle [20], and that this response is also associated with age, sex and training status [21].

Exercise-induced changes in HSPB5 seem to have multiple cyto-protective effects on subcellular components [18,22–24], inhibitory effects on apoptosis [25], as well as a role in the maintenance of enzymatic activity [16], insulin sensitivity and glucose transport [26,27].

Despite the presence of various studies, most of the data focus on single regulatory aspect related to HSPB5 response, mainly by eccentric exercise [21,23,28,29], while the molecular mechanism underlining the HSPB5 modulation induced in mammalian skeletal muscle by physiological, not damaging contraction, remains poorly characterized [22,30].

In the present study, we investigated for the first time different aspects related to HSPB5 regulation in mammalian skeletal muscle after a single bout of non-damaging endurance exercise. Our analysis included expression profile, post-translational modification (i.e. phosphorylation at serine-59), intracellular localization and interaction with substrates and possible client proteins in mouse skeletal muscles also considering the differences in fiber composition. Specifically, we examined at rest and following acute endurance exercise the similarities and differences of HSPB5 modulation by comparing different areas of *Gastrocnemius* muscle with different metabolic properties such as 1) the red *gastrocnemius* (GR), a region of *gastrocnemius* close to others hindlimb posterior muscles (i.e. *plantaris* and *soleus*) with a higher amount of fast twitch oxidative type IIA/X fibers; 2) the white *gastrocnemius* (GW), the outermost portion of the *gastrocnemius* with an exclusive prevalence of fast twitch glycolytic type IIB fibers; 3) the *soleus* (SOL) as reference red muscle, because it has mechanical properties similar to *gastrocnemius* and it is predominantly formed by slow and fast twitch oxidative type fibers. Moreover, to verify the mechanism by which exercise modulates HSPB5, we utilized as *in vitro* model of skeletal muscle C2C12 myocytes exposed to nontoxic H_2O_2 concentration.

2. Materials and methods

2.1. Animals and animal care

Twenty young (7-weeks old) healthy male mice (BALB/c AnNHsd), obtained from Harlan Laboratories (Udine, Italy), were maintained in a 12-h light-dark cycle with free access to food and water. After 1 week of acclimatization to the new housing environment, the mice were familiarized with the Rota-Rod (Rota-Rod; Ugo Basile, Biological Research Apparatus, Comerio Varese, Italy), running 2 days per 10 min. After 1 week, mice were randomly assigned to one of the two experimental groups: control (CTRL) or exercise (EX). The EX mice underwent to an acute bout of endurance exercise, while CTRL mice did not perform any type of exercise. All animal experiments were approved by the Committee on the Ethics of Animal Experiments of the University of Palermo and adhered to the recommendations in the Guide for the Care and Use of Laboratory Animals by the USA National Institute of Health (NIH). All experiments were performed in the Human Physiology Laboratory of the Department of Experimental Biomedicine and Clinical Neurosciences of the University of Palermo, which was formally authorized by the Italian Ministry of Health (Roma, Italy). Experiments conducted before the entry into force of the Decree Law n. 26/2014, in application of the European Directive 2010/63/Eu.

2.2. Single bout of endurance exercise

A motorized Rota-Rod system was used to train the mice. The Rota-Rod is a rotating cylinder on which the mice are forced to run to avoid falling down [31,32]. The exercise (EX) mice ran for 60 min at a speed of 5.5 m/min. Mice were sacrificed immediately, 15, 30 and 120 min after the end of the acute bout of endurance exercise (0′, 15′, 30′ and 120′). Mice were sacrificed by cervical dislocation and the group of posterior muscles (*gastrocnemius* and *soleus*) of the hindlimbs was dissected and preserved in liquid nitrogen (right hindlimb) and embedded in paraffin (left hindlimb) to evaluate the morphological and molecular changes.

2.3. Muscle dissection

The *soleus* and *plantaris* muscles were easily removed pulling the proximal insertions and sectioning the *calcaneal* tendon. In this study the *plantaris* muscle was not analysed. There after the white and the red portion of *gastrocnemius* muscle were separated under microscope according to the muscle color. The red portion (derived from the deep part *gastrocnemius* muscle) and white portion (derived from the superficial part of *gastrocnemius* muscle) have different proportion of red (slow-oxidative) and with fibers (fast-glycolytic). The histological differences between the two portions of *gastrocnemius* muscle have been confirmed previously by our group [33], and further investigated here (Fig. 1). The specimens were immediately cooled in liquid nitrogen and stored at −80 °C for subsequent analyses.

2.4. Immunohistochemistry

Muscles were fixed in a solution of acetone, methanol, and water (2:2:1) for 12 h, washed in tap water and dehydrated with ethanol at 70, 96, 100% v/v. After dehydration, the tissue pieces were placed in xylol for 1.5 h and embedded into paraffin. The embedded muscles were sliced into sections (5 μm) that were mounted on glass slides. For immunohistochemical analysis, the serial sections were incubated in an "antigen unmasking solution" (10 mM tri-sodium citrate, 0.05% Tween-20) for 10 min at 75 °C. Then, the MACH1 kit (M1u539 g, Biocare, Concord, CA, USA) was used according to the manufacturer's instructions. The sections were incubated in primary antibodies, including anti-myosin heavy chain-I (MHC-I, A4951, Hybridoma Bank, Iowa, IA, USA), anti-myosin heavy chain-IIa/IIx (MHC-IIa/IIx, A4.74, Hybridoma Bank, Iowa, IA, USA) or anti-myosin heavy chain-IIb (MHC-IIb, BF-F3, Hybridoma Bank, Iowa, IA, USA), in a humidified chamber overnight at 4 °C. The following day, the sections were incubated for 1 h with the secondary antibody and polymers as previously described [34]. Finally, the slides were cover-slipped, and images were captured with a Leica DM5000 upright microscope (Leica Microsystems, Heidelberg, Germany). By examining serial cross-sections stained for MHC-I and MHC-IIA/X, it was also possible to identify type IIB fibers because of the negative staining.

2.5. Immunofluorescence and confocal analysis

For immunofluorescence, deparaffinized sections were incubated in the "antigen unmasking solution" (10 mM tri-sodium citrate, 0.05% Tween-20) for 10 min at 75 °C, and treated with a blocking solution (3% BSA in PBS) for 30 min. Next, the primary antibody (anti-MHC-I, mouse monoclonal A4.951, Hybridoma Bank; anti-phospho αB-crystallin S59, rabbit polyclonal ab5577, Abcam; anti-β-actin, rabbit polyclonal ab8227, Abcam) diluted 1:50, was applied, and the sections were incubated in a humidified chamber overnight at 4 °C. Then, the sections were incubated for 1 h at room temperature with a conjugated secondary antibody (anti-rabbit IgG–FITC antibody produced in goat, F0382, Sigma-Aldrich; anti-mouse IgG-TRITC antibody produced in goat, T5393, Sigma-Aldrich). Nuclei were stained with Hoechst Stain Solution (1:1,000, Hoechst 33258, Sigma-Aldrich). The slides were treated with PermaFluor Mountant (Thermo Fisher Scientific) and cover slipped. The images were captured using a Leica Confocal Microscope TCS SP8 (Leica Microsystems). Staining intensity for phospho-αB-crystallin of different skeletal muscle fibers was expressed as the mean pixel intensity (PI) normalized to the CSA (cross-sectional area expressed in pixel) using the software Leica application suite advanced fluorescence software as previously described [35].

2.6. Cell culture and treatments

C2C12 mouse myoblasts from ATCC (Manassas, VA) were maintained in Dulbecco's Modified Eagle's Medium (DMEM)/high glucose (Gibco) supplemented with 10% heat-inactivated fetal bovine serum (FBS) and 100 U/mL penicillin/streptomycin (Sigma-Aldrich). Cells were seeded in the growth media and maintained at 37 °C until they achieved 70–80% confluence. Differentiation of myoblasts into myotubes was obtained by replacing growth media with DMEM/high glucose supplemented with 2% FBS and 100U/mL penicillin/streptomycin for 6 days. Cells were grown in a humidified 37 °C incubator (Galaxy S, RSBiotech) with 5% supplemental CO_2 and media were routinely replaced every 2 days. Unless otherwise stated, all experiments were performed using three replicates per treatment.

After 6 days in differentiating medium, myotubes were untreated, treated with hydrogen peroxide for 1 h (H_2O_2 500 μM) alone or in combination with p38MAPK inhibitors (10 μM SB203580 and 10 μM SB239063) (Sigma Aldrich). Inhibitors were added to culture media 1 h before the beginning of H_2O_2 treatment and maintained for whole culture duration. After the treatment, cells were collected immediately (0 h point) or left in fresh culture medium for different recovery periods (3 h, 6 h, 9 h, and 12 h) before collection. To induce cytoskeletal damage, C2C12 myotubes were incubated with 5 μM Cytochalasin D (Sigma Aldrich) for 1 h and then harvested immediately for biochemical analysis.

2.7. Co-immunoprecipitation analysis

C2C12 cells were washed with ice-cold PBS and lysed for 30 min in NP40 lysis buffer (0.5% NP40, 50 mM Tris-HCl, pH 8, 150 mM NaCl, 10% Glycerol) containing protease and phosphatase inhibitor cocktails (Sigma-Aldrich). After centrifugation at 21,500 g for 10 min, the supernatants were subjected to immunoprecipitation.

Firstly, 750 μg of proteins were precleared with 30 μl of Protein G PLUS-Agarose (sc-2002, Santa Cruz) and then the lysate was incubated at +4 °C overnight with 2 μg of primary antibody directed against HSPB5 or phospho-MAPAPK-2 (Thr334). The protein/antibody complexes were then incubated at +4 °C with 40 μl of Protein G PLUS-Agarose (Santa Cruz) for 3 h. Co-immunoprecipitated proteins were subjected to SDS–PAGE analysis, followed by Silver staining gel (SERVA) or western blotting with the indicated antibodies.

2.8. Immuno cytofluorescence

C2C12 cells were fixed with 4% paraformaldehyde/PBS, permeabilized with 1% Triton X-100/TBS for 10 min and washed twice in TBS 1x for 5min.Then samples were blocked in TBS containing 3% BSA for 45min and treated over-night with the following primary antibodies: anti-αBcrystallin (HSPB5), anti-phospho-αBcrystallin (S59) (*p*-HSPB5), diluted 1:100 in TBS containing 0.1% Triton X-100 and BSA 0.1%. Following 3 washes in TBS 1x for 5min, the samples were incubated for 1 h in the dark with the secondary antibodies: Alexa Fluor 488-conjugated donkey anti-goat IgG (Invitrogen) and Alexa Fluor 546-conjugated goat anti-rabbit IgG (Invitrogen), diluted at 1:200. Nuclei were stained with Dapi (Sigma Aldrich). The fluorescent images were captured with a fluorescence microscope (Olympus BX41 microscope, Olympus), which was equipped with a 20× and 40× objectives and corrected for brightness and contrast using conventional software (X-Pro Alexasoft.com 8.03.00).

2.9. Protein extraction and immunoblot analysis

Cells and tissue samples were lysed in RIPA buffer (150 mM NaCl, 50 mM tris-HCl pH8, 1 mM EDTA, 1%NP40, 0.25% sodium deoxycholate, 0.1% SDS), supplemented with protease and phosphatase inhibitor cocktails (Sigma-Aldrich). The determination of protein concentration was measured by colorimetric assay using the BCA protein assay kit (Sigma-Aldrich).

For the immunoblot analysis, an equal amount of proteins (20–30 μg) was resolved in SDS-polyacrylamide gels (10–12%) (BioRad) and transferred onto PVDF membranes (Amersham). Saturated membranes with 5% non-fat dry milk in PBS- Tween (0,01%) were incubated over-night with specific primary antibodies. The immunoreactive protein bands were detected by incubation with horseradish peroxidase-conjugated secondary goat anti rabbit (Millipore) or goat anti mouse (Sigma-Aldrich) antibodies. The Western blot images were acquired on an ImageQuant LAS 4000 (GEHC) and quantified by ImageJ 1.50 h software (National Institute of Health, USA http://imagej.nih.gov/ij). The list of primary antibodies utilized is reported in the Supplementary Table 1.

2.10. Extraction of insoluble and soluble protein pools

To estimate protein partitioning between Triton-soluble (cytosolic) and Triton-insoluble (myofibrillar) fractions of C2C12 cells, a six-well of cultures of differentiated myotubes was washed twice in ice-cold PBS (1 mL) and then scraped in 500 μL. Cells were centrifuged at 12000 × *g* for 10 min at +4 °C and the pellet was lysed in 100 μL detergent-soluble fraction (DSF) buffer containing 10 mM Tris-HCl (pH 7.5), 1% Triton X-100, 5 mM EDTA and supplemented with protease and phosphatase inhibitors cocktail (Sigma). Insoluble material was recovered by a centrifugation at 16000*g* for 15′ at 4 °C. The supernatant (soluble fraction) was collected in new tubes, while the pellet, was then washed with supplemented DSF buffer and centrifuged at 16000 g for 15′ at 4 °C. The insoluble materials represented by pellets were resuspended in 50 μl detergent-insoluble fraction (DIF) buffer enclosing 10 mM Tris-HCl (pH 7.5), 1% SDS and supplemented with protease and phosphatase inhibitors cocktail (Sigma), incubated for 15 min at room temperature and for 2 min on ice, and sonicated once at 50% amplitude for 10 sec on ice (Vibra-Cell, Sonics & Materials). Equal amounts of each fraction were heated for 5 min at 95 °C in 4 × Laemmli Sample Buffer and analysed by SDS-PAGE.

2.11. RNA extraction and RT-qPCR analysis

Total RNA was obtained from muscle tissues or cells using TRIZOL (Invitrogen) according to the manufacturer's procedure. Real-time quantitative RT-PCR was performed on a 7500 Real Time PCR System (Applied Biosystems, Life Technologies). Each 20 μL reaction mixture contained 10 μL of Power SYBR Green RNA-to Ct 1stepMaster mix (2×) (Life Technologies), 10 pmol of specific primer sets, 0.16 μL RT Enzyme Mix (Life Technologies), 10–15 ng of RNA samples. The RT-PCR amplification profile was as follows: RT step at 48 °C for 30 min, followed by enzyme activation at 95 °C for 10 min, and then 40 cycles of denaturation at 95 °C for 15 s and annealing/extension at 60 °C for 1 min. All samples were run in triplicate. The normalization was done utilizing GAPDH or Cyclophilin A as appropriate. A threshold cycle (C_T) was observed in the exponential phase of amplification, and quantification of relative expression levels was performed with standard curves for target genes and the endogenous control. Geometric means were used to calculate the $\Delta\Delta C_T$ (delta-delta C_T) values and expressed as $2^{-\Delta\Delta CT}$. The value of each control sample was set at 1 and was used to calculate the fold-change of target genes. The list of primers utilized is reported in Supplementary Table 2.

2.12. Protein carbonylation analysis

Detection of protein oxidation in muscle lysate and cell culture was performed using the Oxyblot Protein Oxidation Detection Analysis Kit (Millipore, Milano, Italy) according to the manufacturer's protocol. Carbonylated proteins were then resolved on 12% SDS-PAGE and transferred onto a Hybond ECL nitrocellulose membrane (Amersham). Relative intensities of the protein bands were digitally quantified (ImageJ 1.50 h).

2.13. Statistical analyses

All data are presented as group mean ± standard deviation of the mean and analysed by one-way ANOVA with Bonferroni's post-hoc test or Student's *t*-test as appropriate. GraphPad Prism® 5.0a (La Jolla, CA, USA) was used for all statistical analyses, with significant differences determined by $p < 0.05$.

3. Results

3.1. Fiber-types composition analysis of hindlimb skeletal muscle of BALB/c mice

Immunohistochemistry of myosin heavy chains (MHC-I and MHC-IIA/IIX) was performed on serial cross-sections to evaluate the exact fiber composition of each muscle sample (Fig. 1). By overlapping serial cross sections of the same sample stained for MHC-I and MHC-IIA/X, it was also possible to identify type IIB fibers because of the negative staining. In particular, MHC-IIA was the isoform more expressed in SOL (MHC-IIA, 50.75% ± 4.03, $p < 0.01$), followed by MHC-I that was around 42.20% ± 3.70 ($p < 0.01$) (Fig. 1B). Similarly, MHC-IIA was the most expressed isoform in GR (MHC-IIA, 40.25% ± 6.55, $p < 0.01$), while no difference was detected among all other isoforms (MHC-IA, 18.6% ± 4.39; MHC-IIX, 6.75% ± 2.75; MHC-IIB, 15.8% ± 3.35, $p > 0.05$). MHC-IIB was the unique isoform detected in GW (MyHC-IIB, ≈100%) (Fig. 1B).

In term of gene expression, qRT-PCR analysis highlighted that the MyHC-I and MyHC-IIA isoforms were more expressed in SOL compared to all other tissues (MyHC-I, 2953 ± 571; MyHC-IIA, 2077 ± 846, $p < 0.01$), while MyHC-IIX isoform was significantly higher in SOL

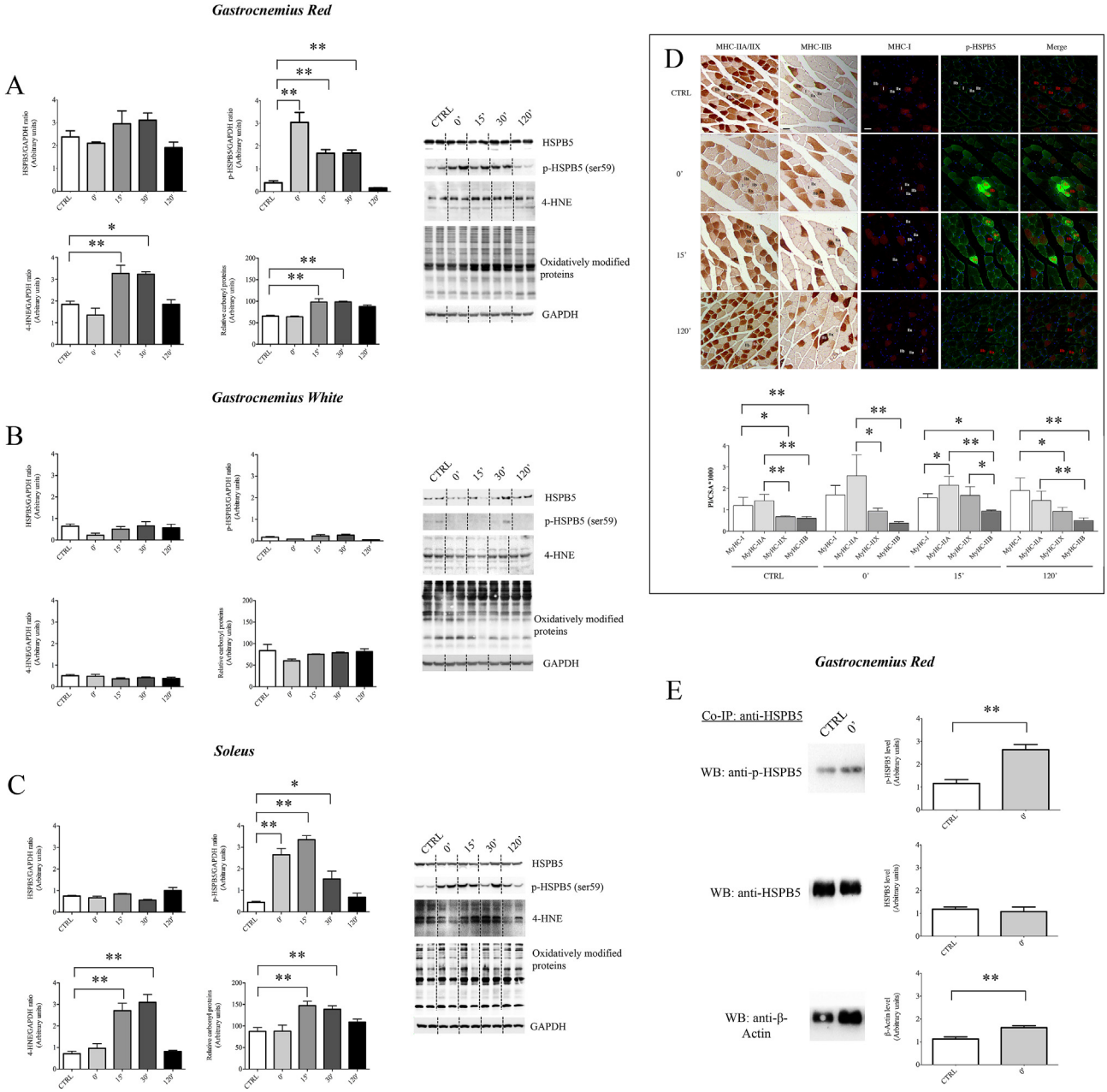

Fig. 2. Densitometric analysis of Western blot related to HSPB5 modulation/activation, signal transduction and oxidative stress proteins in *Gastrocnemius* (**A**) Red, (**B**) White and (**C**) Soleus from control (CTRL) mice and during recovery period after an acute endurance exercise (0′-15′-30′-120′). (**D**) Immunohistochemistry and immunofluorescence for *p*-HSPB5, MHC-I and MHC-IIA/X in serial cross-sections of the whole *gastrocnemius*. Here are showed representative images used for densitometric analysis of the staining intensity. The analysis was performed using 5 fields per section, 5 sections per mice. An average of 435 fibers was analysed for each mouse. The staining intensity of the fibers was expressed as the mean pixel intensity (PI) normalized to the cross-sectional area (CSA) using ImageJ 1.50 h and Leica application suite advanced fluorescence's software. **E**) Western Blot analysis of co-immunoprecipitated proteins of *Gastrocnemius Red* from mice immediately after exercise (0′) showing a band corresponding to HSPB5 that co-immunoprecipitate with *p*-HSPB5 and β-Actin. Data are presented as the means ± SD. Statistical significance was determined using a one-way ANOVA with Bonferroni's post-hoc test or a Student's t-test. **p < 0.01; *p < 0.05.

and GR tissues (MyHC-IIX: SOL, 1900 ± 598; GR, 2174 ± 1143, p < 0.01). Finally, in SOL there was lowest level of MyHC-IIB mRNA expression compared with GR and GW (MyHC-IIB: SOL, 110 ± 78; GR, 11771 ± 2912; GW, 13837 ± 2609, p < 0.01) (Fig. 1C).

3.2. *HSPB5 protein modulation by exercise depends upon fiber composition and correlate to pro-oxidizing environment*

The effects of acute exercise on HSPB5, *p*-HSPB5 and specific oxidative stress markers are shown in Fig. 2. The Western blot analysis in the specific posterior group of hindlimb muscle (i.e. *gastrocnemius* red and white, and *soleus*) did not reveal any significant difference in total HSPB5 protein either between the CTRL and EX groups or within the EX groups at different time points (Fig. 2A–D). However, there was an appreciable difference in the basal levels of HSPB5 and *p*-HSPB5 between muscles. In particular, we found that HSPB5 was significantly more expressed in GR and SOL than in GW (p < 0.05) (Supplementary Fig. 2D). Similarly, at basal level *p*-HSPB5 was more expressed in GR and SOL rather than in GW (p < 0.05). No differences were detected between GR and SOL either for HSPB5 or for its phosphorylated form (Supplementary Fig. 2D). It should be noted that the analysis of HSPB5 content using immunofluorescence approach revealed a different result.

In particular, we detected an increase of reactivity for anti-HSPB5 immediately after endurance exercise (Supplementary Fig. 3).

Acute exercise induced a marked and rapid serine 59 phosphorylation of HSPB5 exclusively in the GR and SOL. Indeed, the content of *p*-HSPB5 was increased significantly already at the end of exercise up to 30 min post exercise ($p < 0.05$) (Fig. 2A and C). At 120 min of recovery, the *p*-HSPB5 levels were similar to CTRL group ($p > 0.05$). No significant induction of the phosphorylated form of this sHSP was observed in the GW ($p > 0.05$) (Fig. 2B). The increase of *p*-HSPB5 was paralleled by the increase in the levels of 4-HNE and carbonyl proteins in GR and SOL at 15 and 30 min of recovery (Fig. 2A–C), whereas no change was observed in GW ($p > 0.05$). At 120 min of recovery, the level of both oxidative stress markers was returned back to values exhibited by CTRL group ($p > 0.05$).

No changes were observed for apoptotic markers (i.e. Bax, Bcl-2 and caspase 3) ($p > 0.05$) (Supplementary Fig. 1), HSPA1A, NFκB-p65 and its phosphorylated form (Supplementary Figs. 1 and 2).

3.3. Effect of exercise on localization of p-HSPB5 within mouse skeletal muscle components

In whole *gastrocnemius* (GS), the detection of *p*-HSPB5 by immunofluorescence showed a mosaic staining patterns with differences in staining intensity between muscle fibers (Fig. 2D). Although the signal was almost undetectable in CTRL mice, *p*-HSPB5 was mostly expressed in MyHC-I and MHC-IIA fibers compared with MHC-IIX and MHC-IIB ($p < 0.01$). Immediately after exercise, MHC-IIA fibers were the isotype more reactive to anti-phospho-HSPB5 with respect to all other fast twitch oxidative and glycolytic isotypes, including MyHC-IIX and MHC-IIB ($p < 0.01$). Already after 15 min of recovery, the cross-sections showed a significantly higher staining intensity for *p*-HSPB5 in MHC-I and MHC-IIA/X ($p < 0.01$). There was no specific staining in MHC-IIB fibers using *p*-HSPB5 antibody ($p > 0.05$). Therefore, these results suggest a preferential response of slow- and fast-twitch oxidative fibers compared with type IIB glycolytic ones.

To explore the interaction between HSPB5 and specific cytoskeletal element, co-immunoprecipitates from GR of CTRL and exercised (0′) mice using anti-HSPB5 antibody were further probed with anti-*p*-HSPB5 and anti-β-actin. As expected, both *p*-HSPB5 and β-actin were detected in the immunoprecipitated proteins. In particular, there was ≈2.2 increase of *p*-HSPB5 and ≈1.4 fold increase of β-actin in GR immediately after the single bout of exercise (Fig. 2E).

3.4. Modulation of HSPB5 in C2C12 myotubes exposed to reactive oxygen species

Differentiation of C2C12 cells was confirmed by their morphological changes as well as the expression of specific adult MyHC isoforms (type I, IIA, IIX and IIB) [36] (Fig. 3A–C). Importantly, the content in MyHC isoforms in C2C12 cells described here at both protein and the mRNA levels was in agreement with the result reported by previous *in vivo* and *in vitro* studies [36,37], suggesting that this cell line is a good model to study fast muscles such as *extensor digitorum longus*, *plantaris* and *gastrocnemius*.

In order to understand the role of HSPB5 in skeletal tissue during muscle contraction, we exposed C2C12 myotubes to non-cytotoxic dose of H_2O_2 being the increase in reactive oxygen species (ROS) an essential but not unique component of the multifactorial stress generated by acute endurance exercise. Preliminary results showed that the exposure of C2C12 myotubes to 500 μM of H_2O_2 was well tolerated, without induction of apparent morphological modifications (data not shown) and no significant changes in the expression of stress-responsive proteins related to the apoptotic pathway, such, Bax, Bcl-2 and caspase 3 (Supplementary Fig. 1D). Irrespective from the recovery time period, the Western Blot analysis showed unchanged levels of total HSPB5 protein after 1 h of H_2O_2 exposure ($p > 0.05$) (Fig. 3D–E). Differently, it revealed a striking increase in *p*-HSPB5 already immediately after the treatment ($p < 0.01$), remaining significantly higher compared with untreated myotubes up to 9 h of recovery ($p < 0.05$) (Fig. 3D–E). As expected, the transcript levels for HSPB5 gene remained unchanged over the different recovery periods ($p > 0.05$) (Fig. 3F). In light of these results, 3 h of recovery time was chosen as experimental point to set all next protocols.

Immunostaining analysis of HSPB5 was performed on C2C12 myotubes exposed to ROS and, as shown in Fig. 3G, there was not difference in the level of HSPB5 between control and treated cells, while there was an appreciable increase of *p*-HSPB5 following H_2O_2 exposure (Fig. 3H). No immunoreactivity was observed in cells incubated solely with the respective secondary antibodies (data not shown).

3.5. Analysis of cellular pathway related to HSPB5 phosphorylation, localization and functional interaction

Similarly to the features analysed in GR and SOL muscles, the increase in *p*-HSPB5 induced in C2C12 myotubes by 500 μM of H_2O_2 was paralleled by a significant increase of 4-HNE ($p < 0.01$) and carbonylated proteins ($p < 0.05$), while no modulation was found for HSP1A ($p > 0.05$) (Fig. 4A).

Being p38MAPK able to integrate various stress signals, including those induced by ROS, from the cellular environment and conveying these signals to the cytoplasm and nucleus by phosphorylating a variety of substrates, we checked for p38MAPK modulation in muscle tissues from mice at rest and following exercise, but we did not identify any changes of p38MAPK and phospho-p38MAPK (p-p38MAPK) in total GR, GW and SOL protein extracts (Supplementary Fig. 4). Similarly, myotubes exposed to H_2O_2 for 1 h did not show any modulation of both p38MAPK and p-p38MAPK at any recovery point time (Fig. 4B). However, a pre-treatment of C2C12 with both SB239063 and SB203580, two selective inhibitors of p38MAPK activity, induced a consistent decrease of both p-p38MAPK and *p*-HSPB5 (Fig. 4C). Moreover, under the same culture condition, myotubes exposed to pro-oxidant showed an increased content of the downstream target of p-38MAPK, the MAPK-activate protein kinase 2 (*p*-MAPKAPK2), compared with control cells ($p < 0.05$) (Fig. 4D).

The results from the cellular fractionation protocols showed that, after the H_2O_2 treatment, HSPB5 translocates in the insoluble fraction of C2C12 myotubes, where it appears to be manly phosphorylated (Fig. 5A). The presence of both p38MAPK inhibitors reduces significantly the amount of HSPB5 phosphorylated, confirming a direct role of p38MAPK in the phosphorylation of HSPB5 under oxidative stress conditions. However, these results were not consistent with phosphorylation causing redistribution of this sHSP between compartments (Fig. 5B). A similar result was observed when the cells were exposed to cytochalasin D, a well-known cytoskeletal stressor (Fig. 5C), suggesting a common modulation of HSPB5 in response to different cellular perturbation impacting the cytoskeletal network.

The silver staining analysis of the proteins extracted by C2C12 myotubes cultured in presence or not of pro-oxidant stimulus (H_2O_2) and co-immunoprecipitated with an anti-HSPB5 antibody showed either the presence of new bands or an increased staining of bands already present in untreated cells (Fig. 5D). When these proteins were immunoblotted with antibodies targeting selected known and/or putative molecular interactors, we detected the presence of *p*-HSPB5, β-actin, pro-caspase 3, desmin and filamin1, whose relative concentration in the precipitate was differently modulated by H_2O_2 and/or p38MAPK inhibitors. Differently from β-actin, marginally modulated by the pro-oxidant environment and by HSPB5 phosphorylation, the interaction between HSPB5 with pro-caspase 3, desmin and the new identified interactor filamin1 resulted enhanced by H_2O_2 treatment and negatively modulated by p38MAPK inhibitors (Fig. 5E).

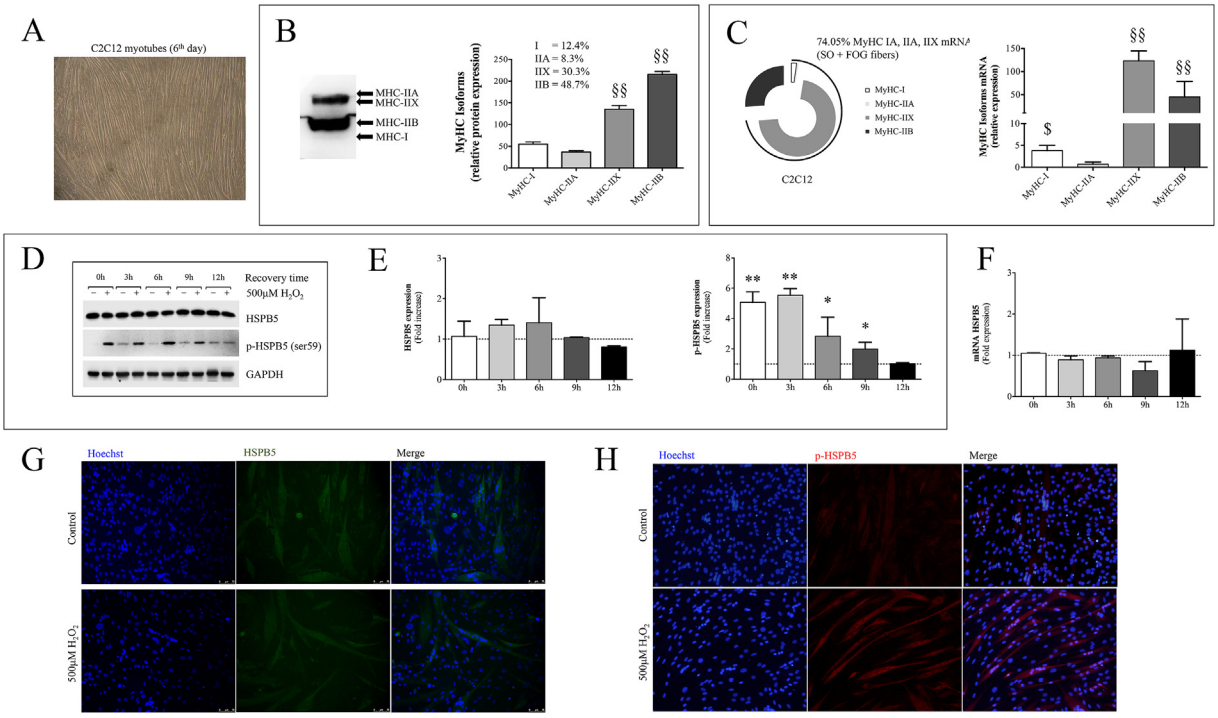

Fig. 3. (**A**) C2C12 myotubes at 6th day in differentiation medium. (**B**) A representative Western blot showing the protein levels of MyHC isoforms from C2C12 myotubes. (**C**) qRT-PCR analysis. The percentage of MyHC isoforms expression is shown as exploded doughnut. Bar diagram shows the relative expression of mRNA MyHC isoforms. In **D** and **E** whole-cell extracted by myotubes treated with 500 μM H_2O_2 for 1 h and collected at indicated recovery times were immunoblotted with antibodies against HSPB5, *p*-HSPB5 (Ser59). The quantification of each protein level was relative to GAPDH and represented as fold change. **F**) HSPB5 mRNA expression level was carried out at the same experimental points of protein expression analysis and represented as fold change (mean ± SD, $n = 3$). Myotubes treated with H_2O_2 and collected after 3 h were also fixed and immunoblotted with primary and secondary antibodies to detect total HSPB5 protein (**G**) and its phosphorylated form (*p*-HSPB5) (**H**). Hoechst nucleic acid stain was utilized to display nuclei. Scale bars = 75μM. Data are presented as the means ± SD ($n = 3$). Statistical significance was determined using either a one-way ANOVA with Bonferroni's post-hoc test or *t*-test analysis. §§p < 0.01 *vs.* MyHC-I and MyHC-IIA; $p < 0.05 *vs.* MyHC-IIA; **p < 0.01 *vs.* CTRL level; *p < 0.05 *vs.* CTRL level. **SO**, Slow Oxidative fibers; **FOG**, Fast Oxidative-Glycolytic fibers. (————) CTRL level.

4. Discussion

The application of molecular biology techniques to exercise biology has proven a better understanding of the multiplicity and complexity of cellular pathways by which exercise training can prevent or ameliorates the progression of many physio-pathological conditions [38–40]. In the past, several research groups have shown as a regular physical activity can induce a significant enhancement in muscular and functional performance, cardiovascular health, as well as a beneficial anti-aging systemic effect through the modulation of redox homeostasis and/or stress-response proteins [33,34,41–47].

Considering that muscle HSPB5 is highly modulated by exercise, showing special cytoprotective properties towards damaged and/or stressed cytoskeleton components during ischemia or exercise [15,48], we were interested in ascertaining a) the early response of HSPB5 protein in skeletal muscle to an acute bout of non-damaging exercise in relation to fiber-type composition, subcellular localization and substrate interaction and b) the role of HSPB5 phosphorylation and/or pro-oxidant environment in this response. To this aim, both *in vivo* exercise protocol and *in vitro* pro-oxidant environment were designed to avoid cellular damage and the risk of contamination caused by inflammatory processes or sarcomere disruption.

The *gastrocnemius* was utilized to obtain, from the same muscle, two distinct regions in term of fibers composition: red *gastrocnemius*, as source of slow-oxidative and fast glycolytic/oxidative, and white *gastrocnemius*, as source of fast-glycolytic fibers. We also utilized the *soleus,* a muscle tissue mainly composed by slow oxidative type fibers, which has a similar function of the *gastrocnemius* and belong to the same muscle group utilized for running, called “Calf muscles”. The fiber-type distribution found here in BALB/c mice muscles not only confirmed substantial differences among SOL, GR and GW but it likely suggests a different aerobic capacity/long-duration activity, which decreases orderly from SOL to GR, reaching lowest level in GW [49,50].

Skeletal muscle contractions result in an increased generation of ROS that, potentially harmful at high concentration, hold a fundamental role in muscle adaptation to exercise training [51]. Muscle cells have very efficient antioxidant defence systems to buffer the production of ROS [52], as well as stress response proteins, such as HSPs, to counteract ROS-related modifications to biomolecules [53]. Lipid peroxidation and protein carbonylation, that occurs either by direct interaction with ROS or indirectly through lipid peroxidation, is a particularly susceptible process generating uniquely modified molecules that can be used as “fingerprints” to detect the shift of cell environment towards a pro-oxidant state in different conditions, like physical exercise, aging or diseases [54–58].

Considering the differences in fibers composition and in their related metabolic properties [50], which determine a different aerobic capacity/long-duration activity of the muscle tissues selected [49], it was not surprising that the analysis of lipid peroxidation and protein carbonylation after acute exercise revealed a significant increase only in SOL and GR, muscles with a consistent percentage of oxidative fiber types. Compared to glycolytic fibers, the higher mitochondrial density and activity of oxidative fibers determine a higher ROS production [59] and a higher susceptibility to ROS-mediated alterations [60]. The lack of any significant change in the NFκB, NFκB (p65) phosphorylation and apoptotic markers following exercise, verified the not damaging feature of the muscle contraction and the cell sustainability of the exercise-mediated oxidative stress, possibly occurring below the threshold levels

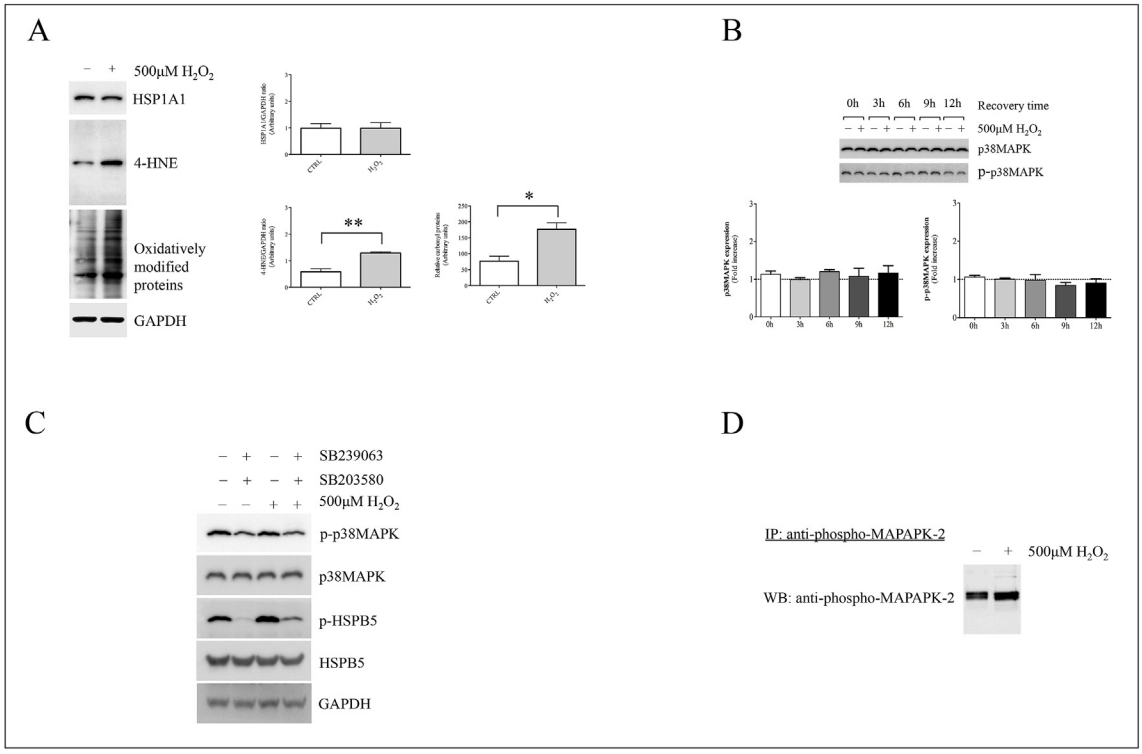

Fig. 4. (**A**) Analysis of HSP1A1, 4-HNE, and oxidatively modified proteins content in C2C12 myotubes treated with H_2O_2. The quantification of each protein level was relative to GAPDH. Oxidatively modified proteins were determined by oxyblot analysis. Data are presented as the means ± SD ($n = 3$). (**B**) Densitometric analysis of Western blot related to p-38MAPK and p-p38MAPK in whole-cell extracted by myotubes treated with H_2O_2 and collected at indicated recovery times. Data were represented as fold change mean ($n = 3$). **C**) Fully differentiated myotubes were also treated with H_2O_2, in presence or not of both pharmacological inhibitors of p38MAPK (SB239063 and SB203580), to analyse the protein levels of p38MAPK, HSPB5 and their phosphorylated forms. **D**) Immunoprecipitation analysis of phospho-MAPAPK-2 in C2C12 myotubes exposed to pro-oxidant environment. (————) CTRL level. Unless different indicated, C2C12 cells were treated with H_2O_2 for 1 h followed from 3 h of recovery. Statistical significance was determined using either a one-way ANOVA with Bonferroni's post-hoc test or Student's t-test. **p < 0.01 *vs.* CTRL; *p < 0.05 *vs.* CTRL.

of cellular defence systems, and not sufficient to cause further detrimental effects and cell death [61].

It is well known that the increased ROS production generated by exercise, besides other adaptative response, is also involved in the induction of sHSPs [43,62]. The biological role of these proteins is mainly to act as "holdase", interacting with partly or completely unfolded proteins in the early phase of stress response and then facilitating their refolding through the "foldase" activity of other HSPs [19]. In this work, we confirm that the basal levels of HSPB5 and its phosphorylated form is different between slow-twitch and in fast-twitch muscle fibers [63].

Differently from the results obtained by immunoblotting analyses, we detected an increase of reactivity for anti-HSPB5 immediately after endurance exercise when analysing tissue samples by immunofluorescence approach. We hypothesize that the acute exercise might promote the transition of HSPB5 from a low-to a high-affinity status presumably reducing the oligomer size, thus determining a major exposure of epitopes detected by antibody, previously engaged in high-order of oligomers [64,65].

There is evidence that, following stresses, a certain portion of HSPB5 pool becomes phosphorylated and correlatively shows an enhanced affinity for the various elements of the cell [66,67]. The fiber-type specific levels of *p*-HSPB5 in skeletal muscle following endurance exercise represent a novel finding: we showed that phosphorylation levels of this sHSP were significantly increased only in skeletal muscle with a higher amount of type I and IIA/X myofibers. In particular, the level of *p*-HSPB5 was apparently in proportion with the percentage of type I and IIA/X myofibers contained in slow twitch and mixed muscles (i.e., SOL, GR). In support of the aforementioned data, serial cross-sections of the muscles revealed that the phosphorylated form of HSPB5 was significantly elevated after exercise only in type I, IIA, and IIX muscle fiber, while type IIB fibers appeared not specifically positive for *p*-HSPB5. The quantitative distribution pattern of *p*-HSPB5 detected by immunohistochemistry was confirmed by means of a quantitative computational analysis performed at individual muscle fiber level. Considering the results on lipid peroxidation and protein carbonylation, we hypothesized that the differential HSPB5 response in different muscle fiber types could reflect differences in the level of oxidation that occurred with exercise. This might involve differences in the rate of production of ROS and/or reactive nitrogen species (RNS) or in the types of ROS and RNS that accumulate during exercise. Moreover, the different susceptibility of various protein isoforms to oxidation by ROS and/or RNS, could also explain the different fiber type-specific HSPB5 responses we observed, since the downstream effects of oxidative stress may act as the signal for a modulation of HSPB5 phosphorylation with exercise [51,68]. This highly specific response of muscle fiber to acute exercise could help to explain previous finding that show a training adaptation occurred only within GR rather that GW [69,70] as well as to reinforce the idea that the phosphorylation of HSPB5 in these tissues possibly reflects the level of stress experienced by the muscle.

Considering that the translocation to cytoskeletal components is one of the prime step in the cellular defence system mediated by HSPB5 [71], we were interested to verify the relevance of protein phosphorylation in HSPB5 translocation from the cytosol to the myofibrillar subcellular fraction, as well as in the interaction with specific substrates. In GR, we found that the increase in the β-actin that co-immunoprecipitated together with HSPB5 after exercise was related to an increase in *p*-HSPB5. Therefore, a single bout of endurance exercise induced a rapid phosphorylation of HSPB5, likely reduced its oligomer size and increased its affinity for the β-actin and possibly other

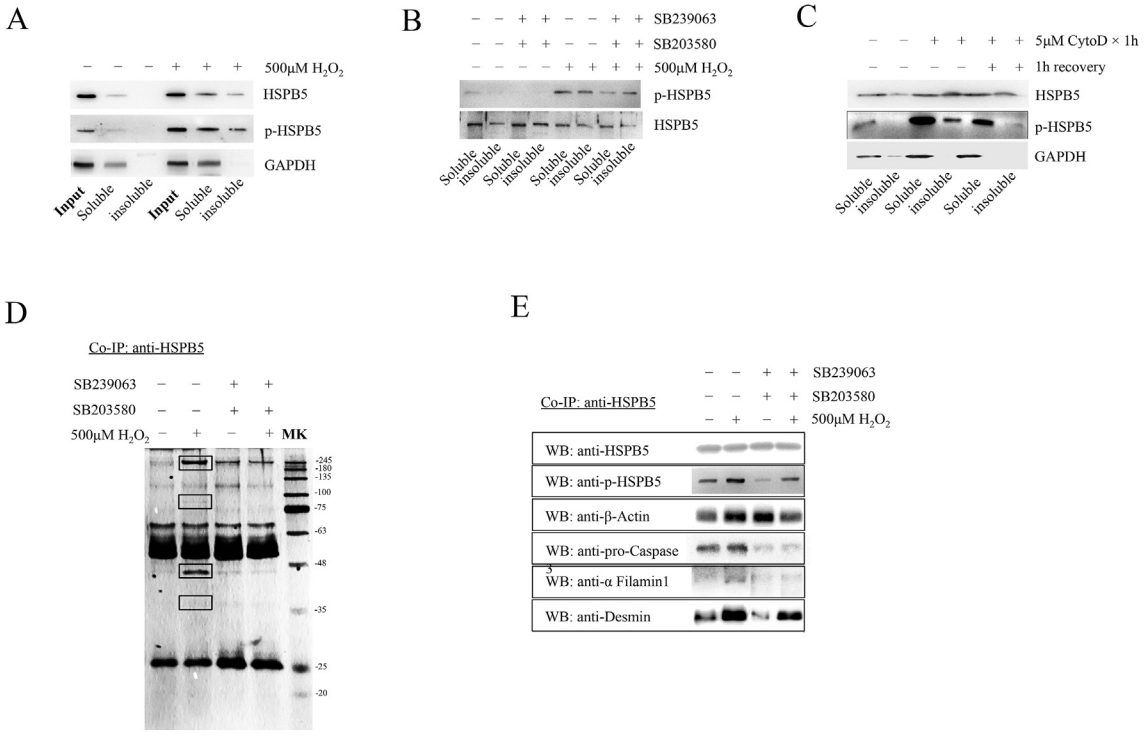

Fig. 5. In (**A**) and (**B**) C2C12 myotubes were exposed to pro-oxidant and to p38MAPK inhibitors were fractionated into insoluble and soluble protein pools. Solubilized lysates were then separated by SDS-PAGE and analysed for HSPB5 and *p*-HSPB5 levels. **C**) Both whole and fractionated pools of proteins were obtained from myotubes exposed to cytochalasin D for 1 h and also followed a period of recovery. Soluble and insoluble fraction were analysed for HSPB5 and *p*-HSPB5 content. Whole proteins extracted from C2C12 myotubes treated with H_2O_2 in presence or not of both pharmacological inhibitors of p38MAPK were firstly co-immunoprecipitated for HSPB5 and then both **D**) visualized on gel staining the proteins with silver nitrate and **E**) analysed through SDS-PAGE for the indicated antibodies. Unless different indicated, C2C12 cells were treated with H_2O_2 for 1 h followed from 3 h of recovery.

myofibrillar proteins [65,72].

In the past, it has been demonstrated that C2C12 myotubes possess most of the morpho-functional features of contractile muscle cell and, therefore, they are considered a reliable *in vitro* model to study at molecular level the physiopathology of several skeletal muscle tissues such as *Gastrocnemius*, *EDL* and *plantaris* [36,73,74]. In fact, as suggested by others [37,75,76], C2C12 myotubes are not intrinsically committed to form distinct types of fast and slow MHC-expressing myotubes, but they are elongated syncythia with numerous nuclei expressing more than one MHC isoform. In particular, we showed at protein and transcript level that the expression pattern of MHC isoforms includes more than 51% of slow oxidative and fast oxidative-glycolytic isoforms (i.e., IA, IIA/X).

Physical exercise can produce various homeostatic perturbations, including mechanical, thermal and oxidative stress [77]. However, the exposure of cultured myotubes to mild, non-cytotoxic ROS concentration reproduces *in vitro* one of the main stimuli linked to the process of homeostasis and adaptation induced by the exercise in skeletal muscle [78] and trigger and/or impact many signalling pathways similar to those observed *in vivo* through exercise. In particular, to verify that the pro-oxidant environment is a key modulator for the HSPB5 response induced by acute endurance exercise in skeletal muscle [43,51,62,79], we analysed the effect of non-toxic H_2O_2 concentrations in C2C12 mouse myotubes.

The exposure of C2C12 to hydrogen peroxide *in vitro* induced a cellular response similar to that induced in GR and SOL muscles by exercise *in vivo*. Specifically, we found that while HSPB5 levels were not modulated either at protein or at RNA levels, the amount of *p*-HSPB5 was significantly increased immediately after H_2O_2 treatment up to 9 h after the end of the treatment. In respect to the signalling pathways mediating this effect, a plethora of studies point to the intermediation of p38MAPK in Ser59 phosphorylation [80–82]. Indeed, p38MAPK is stimulated by different stressors, such as heat shock or oxidative stress, and is also considered the major kinase involved in sHSPs' signalling pathway. Differently from previous research conducted on proliferating muscle cells [81], we were unable to verify an oxidative-related increase of p-p38MAPK level in our *in vivo* and *in vitro* protocols. Nevertheless, using a mix of two selective pharmacological p38MAPK inhibitors (SB239063 and SB203580), we found that p38MAPK and its downstream substrate MAPKAPK2 could be involved in H_2O_2- and, very similarly, in exercise-induced HSPB5 (Ser59) phosphorylation [83,84]. Although we cannot exclude the involvement of cyclin AMP-dependent/PKA and calcium signalling pathways [85,86], we hypothesized that, as already described for HSPB1 [87], the disturbance of cell homeostasis generated during our experimental conditions could result in 1) a very early p38MAPK activation within exercise protocol or cell treatments and/or 2) the activation of convergent pathways to p38MAPK and/or 3) that basal levels of p-p38MAPK are sufficient to activate the downstream signalling pathways, which results in the phosphorylation of HSPB5.

It has been suggested that serine 59 phosphorylation in HSPB5 shifts the distribution of higher-order oligomers towards smaller species, which have a greater ability to bind specific targets, and thus, an increased chaperone activity [65]. To explore the biological function of the phosphorylated form of HSPB5, we analysed the protein localization using cellular fractionation protocol and then through immunoblotting analysis for a phospho-specific anti-HSPB5 (Ser59) antibody.

The presence of both p38MAPK inhibitors in C2C12 cultures not only reduced significantly the amount of H_2O_2-induced *p*-HSPB5, but also suggested that the HSPB5 phosphorylation occurs in both compartments to a fairly similar degree and that this modification was not consistent with the redistribution of HSPB5 between compartments. Similar results were observed when the microfilament architecture was

disturbed with cytochalasin D, a molecule able to affect actin polymerization by capping the barbed end of actin filaments. Therefore, it is likely that our experimental condition produces a physiological stress at cytoskeletal level that induces the phosphorylation of HSPB5 and, thereby its enhanced affinity for various elements of the cytoskeleton. It has been described that HSPB5 interacts with proteins involved in apoptotic pathway, such as cytochrome c, Bcl-2 and pro-caspase 3 [66,67], as well as to proteins of microtubules, microfilaments and intermediate filaments of cytoskeleton networks such as actin, desmin, titin and tubulin [81]. Following exposure to oxidative stress, we found that HSPB5 co-immunoprecipitated with targets already known such as β-actin, desmin and pro-caspase 3. Further, we show for the first time that HSPB5 co-immunoprecipitated with α-Filamin 1 (Filamin A, FLNA) and that the interaction between these two proteins was modulated by phosphorylation. Filamins are actin-crosslinking proteins consisting of an N-terminal actin binding domain (ABD) followed by 24 immunoglobulin-like repeats [88] and they are involved in a number of cellular processes including cell-matrix adhesion, mechanoprotection and actin remodelling [89,90]. There are three filamin homologues: filamin A (FLNA), filamin B (FLNB) and C (FLNC). Filamin A and B are both ubiquitously expressed, whereas filamin C is specifically expressed in skeletal and cardiac muscle [88]. In agreement with our finding, the *Drosophila* HSPB5, known as l(2)efl, has been identified to be required for Z-band pattering and might maintain myofibrillar integrity through interacting with Cheerio, the homolog of human filamin [91]. Moreover, it has been demonstrated that other mammalian sHSP, such as HSPB7, binds to FLNA and FLNC, and translocate from the cytosol to myofibrils during muscle ischemia to maintain normal functioning of skeletal muscle [48]. These results cannot exclude that HSPB5/p-HSPB5 binds to other members of this family proteins, but they highlight as under oxidative stress condition *p*-HSPB5 might specifically maintain muscle integrity stabilizing the interaction of FLNA. Further studies including pull-down analysis and other proteomic approach are required to define the direct interaction between these proteins as well as the intriguing network of HSPB5′ substrates and clients.

5. Conclusion

In this study, we provide a new piece of the skeletal muscle response mechanism to a non-damaging acute endurance exercise suggesting also a potential explanation of the process by which HSPB5 could protect structural and functional proteins from contraction-induced oxidative stress. Our findings offer compelling evidences indicating that i) *p*-HSPB5 is distributed in a fiber-type specific pattern and its increase upon acute aerobic exercise is correlated with increased levels of both lipid peroxidation and protein carbonylation, not related to cell damage or apoptosis activation; ii) HSPB5 phosphorylation under pro-oxidant stimuli is likely depending from an early activation of the p38MAPK pathway, which facilitate in different way the HSPB5′ interaction with functional and structural proteins known to be essential for muscle fiber integrity and survival. In particular, we confirmed the role of HSPB5 phosphorylation in the interaction with pro-caspase 3, desmin, and the protein α-Filamin 1 (Filamin A or FLNA), identified here for the first time as a new HSPB5 substrate. Although the possible role of the phosphorylation on HSPB5 re-localization still remains unresolved, our data reinforce the idea that the phosphorylation of HSPB5 in these tissues possibly reflects the level of stress that the muscle experienced. Indeed, an exercise lasting the same time but at a lower velocity neither changed the antioxidant status nor modulated HSPB5 in skeletal muscles of mice (data not shown).

Given the importance of HSPB5 in many another tissues and by the variety of diseases where the expression of this protein is deregulated, we strongly believe that a deep understanding of the role of HSPB5 during physiological stimuli could be important for future studies to identify new therapeutic strategies based on HSPB5 to prevent or treat most of the pathological conditions where this protein is involved.

Conflicts of interest

The authors declare that there are not conflicts of interest.

Funding

This work was supported by “Ministero dell’Istruzione, dell’Università e della Ricerca” (MIUR), Italy (PRIN2012-prot. 2012N8YJC3 to Daniela Caporossi and Felicia Farina) and by University of Rome "Foro Italico", Italy (Research Grant CDR2.RIC182015).

Appendix A. Supplementary data

Supplementary data to this article can be found online at https://doi.org/10.1016/j.redox.2019.101183.

References

[1] F.U. Hartl, A. Bracher, M. Hayer-Hartl, Molecular chaperones in protein folding and proteostasis, Nature 475 (2011) 324–332.
[2] R. Bakthisaran, R. Tangirala, C.M. Rao, Small heat shock proteins: role in cellular functions and pathology, Biochim. Biophys. Acta 1854 (4) (2015) 291–319.
[3] E. Thornell, A. Aquilina, Regulation of αA- and αB-crystallins via phosphorylation in cellular homeostasis, Cell. Mol. Life Sci. 72 (2015) 4127–4137.
[4] I.J. Benjamin, J. Shelton, D.J. Garry, J.A. Richardson, Temporospatial expression of the small HSP/alpha B-crystallin in cardiac and skeletal muscle during mouse development, Dev. Dynam. 208 (1997) 75–84.
[5] J.P. Brady, D.L. Garland, D.E. Green, E.R. Tamm, F.J. Giblin, E.F. Wawrousek, AlphaB crystallin in lens development and muscle integrity: a gene knockout approach, Investig. Ophthalmol. Vis. Sci. 42 (2001) 2924–2934.
[6] I. Dimauro, L. Grasso, S. Fittipaldi, C. Fantini, N. Mercatelli, S. Racca, S. Geuna, A. di Gianfrancesco, D. Caporossi, F. Pigozzi, P. Borrione, Platelet-rich plasma and skeletal muscle healing: a molecular analysis of the early phases of the regeneration process in an experimental animal model, PLoS One 9 (7) (2014) e102993.
[7] J.P. Fichna, A. Potulska-Chromik, P. Miszta, M.J. Redowicz, A.M. Kaminska, C. Zekanowski, S. Filipek, A novel dominant D109A CRYAB mutation in a family with myofibrillar myopathy affects αB-crystallin structure, BBA Clin. 7 (2016 Nov 11) 1–7.
[8] R.L. Neppl, M. Kataoka, D.Z. Wang, Crystallin-αB regulates skeletal muscle homeostasis via modulation of argonaute 2 activity, J. Biol. Chem. 289 (24) (2014 Jun 13) 17240–17248.
[9] N.S. Rajasekaran, P. Connell, E.S. Christians, L.J. Yan, R.P. Taylor, A. Orosz, X.Q. Zhang, T.J. Stevenson, R.M. Peshock, J.A. Leopold, W.H. Barry, J. Loscalzo, S.J. Odelberg, I.J. Benjamin, Human alpha B-crystallin mutation causes oxido-reductive stress and protein aggregation cardiomyopathy in mice, Cell 130 (3) (2007 Aug 10) 427–439.
[10] S. Sacconi, L. Féasson, J.C. Antoine, C. Pécheux, R. Bernard, A.M. Cobo, A. Casarin, L. Salviati, C. Desnuelle, A. Urtizberea, A novel CRYAB mutation resulting in multisystemic disease, Neuromuscul. Disord. 22 (1) (2012 Jan) 66–72.
[11] P. Vicart, A. Caron, P. Guicheney, Z. Li, M.C. Prévost, A. Faure, D. Chateau, F. Chapon, F. Tomé, J.M. Dupret, D. Paulin, M. Fardeau, A missense mutation in the alphaBcrystallin chaperone gene causes a desmin-related myopathy, Nat. Genet. 20 (1998) 92–95.
[12] T. Iwaki, A. Iwaki, J.E. Goldman, aB-crystallin in oxidative muscle fibers and its accumulation in ragged-red fibers: a comparative immunohistochemical and histochemical study in human skeletal muscle, Acta Neuropathol. 85 (1993) 475–480.
[13] P. Doran, J. Gannon, K. O'Connell, K. Ohlendieck, Aging skeletal muscle shows a drastic increase in the small heat shock proteins alphaB-crystallin/HspB5 and cvHsp/HspB7, Eur. J. Cell Biol. 86 (2007) 629–640.
[14] S. Fittipaldi, N. Mercatelli, I. Dimauro, M.J. Jackson, M.P. Paronetto, D. Caporossi, Alpha B-crystallin induction in skeletal muscle cells under redox imbalance is mediated by a JNK-dependent regulatory mechanism, Free Radic. Biol. Med. 86 (2015) 331–342, https://doi.org/10.1016/j.freeradbiomed.2015.05.035.
[15] T.J. Koh, J. Escobedo, Cytoskeletal disruption and small heat shock protein translocation immediately after lengthening contractions, Am. J. Physiol. Cell Physiol. 286 (2004) C713–C722.
[16] G.C. Melkani, A. Cammarato, S.I. Bernstein, αBcrystallin maintains skeletal muscle myosin enzymatic activity and prevents its aggregation under heat-shock stress, J. Mol. Biol. 3 (2006) 635–645.
[17] P.D. Neufer, G.A. Ordway, R.S. Williams, Transient regulation of c-fos, alpha B-crystallin, and hsp 70 in muscle during recovery from contractile activity, Am. J. Physiol. 274 (2 Pt 1) (1998 Feb) C341–C346.
[18] G. Paulsen, K. Vissing, J.M. Kalhovde, I. Ugelstad, M.L. Bayer, F. Kadi, P. Schjerling, J. Hallen, T. Raastad, Maximal eccentric exercise induces a rapid accumulation of small heat shock proteins on myofibrils and a delayed HSP70 response in humans, Am. J. Physiol. Regul. Integr. Comp. Physiol. 293 (2007) R844–R853.
[19] I. Dimauro, A. Antonioni, N. Mercatelli, D. Caporossi, The role of αB-crystallin in skeletal and cardiac muscle tissues, Cell Stress Chaperones 23 (4) (2018 Jul) 491–505, https://doi.org/10.1007/s12192-017-0866-x.
[20] E.G. Noble, K.J. Milne, C.W. Melling, Heat shock proteins and exercise: a primer,

Appl. Physiol. Nutr. Metabol. 33 (5) (2008 Oct) 1050–1065, https://doi.org/10.1139/H08-069.
[21] M. Folkesson, A.L. Mackey, H. Langberg, E. Oskarsson, K. Piehl-Aulin, J. Henriksson, F. Kadi, The expression of heat shock protein in human skeletal muscle: effects of muscle fibre phenotype and training background, Acta Physiol (Oxf). 209 (1) (2013 Sep) 26–33, https://doi.org/10.1111/apha.12124.
[22] K.T. Cumming, G. Paulsen, M. Wernbom, I. Ugelstad, T. Raastad, Acute response and subcellular movement of HSP27, αB-crystallin and HSP70 in human skeletal muscle after blood-flow-restricted low-load resistance exercise, Acta Physiol (Oxf). 211 (2014) 634–646, https://doi.org/10.1111/apha.12305.
[23] N.T. Frankenberg, G.D. Lamb, K. Overgaard, R.M. Murphy, K. Vissing, Small heat shock proteins translocate to the cytoskeleton in human skeletal muscle following eccentric exercise independently of phosphorylation, J. Appl. Physiol. 116 (2014) 1463–1472.
[24] G. Paulsen, F. Lauritzen, M.L. Bayer, J.M. Kalhovde, I. Ugelstad, S.G. Owe, J. Hallén, L.H. Bergersen, T. Raastad, Subcellular movement and expression of HSP27, alphaB-crystallin, and HSP70 after two bouts of eccentric exercise in humans, J. Appl. Physiol. 107 (2) (2009 Aug) 570–582, https://doi.org/10.1152/japplphysiol.00209.2009 1985.
[25] V.L. Gabai, M.Y. Sherman, Interplay between molecular chaperones and signaling pathways in survival of heat shock, J. Appl. Physiol. 92 (2002) 1743–8.
[26] P.A. Kumar, A. Haseeb, P. Suryanarayana, N.Z. Ehtesham, G.B. Reddy, Elevated expression of alphaA- and alphaB-crystallins in streptozotocin-induced diabetic rat, Arch. Biochem. Biophys. 444 (2005) 77–83.
[27] D.J. Toft, M. Fuller, M. Schipma, F. Chen, V.L. Cryns, B.T. Layden, αB-crystallin and HspB2 deficiency is protective from diet-induced glucose intolerance, Genom Data 9 (2016 May 13) 10–17.
[28] L. Féasson, D. Stockholm, D. Freyssenet, I. Richard, S. Duguez, J.S. Beckmann, C. Denis, Molecular adaptations of neuromuscular disease-associated proteins in response to eccentric exercise in human skeletal muscle, J. Physiol. 543 (Pt 1) (2002 Aug 15) 297–306.
[29] G. Paulsen, K.E. Hanssen, B.R. Rønnestad, N.H. Kvamme, I. Ugelstad, F. Kadi, T. Raastad, Strength training elevates HSP27, HSP70 and αB-crystallin levels in musculi vastus lateralis and trapezius, Eur. J. Appl. Physiol. 112 (5) (2012 May) 1773–1782, https://doi.org/10.1007/s00421-011-2132-8.
[30] J.P. Morton, D.P.M. MacLaren, N.T. Cable, T. Bongers, R.D. Griffiths, I.T. Campbell, L. Evans, A. Kayani, A. McArdle, B. Drust, Time course and differential responses of the major heat shock protein families in human skeletal muscle following acute nondamaging treadmill exercise, J. Appl. Physiol. 101 (2006) 176–182.
[31] R. Barone, M. Bellafiore, V. Leonardi, G. Zummo, Structural analysis of rat patellar tendon in response to resistance and endurance training, Scand. J. Med. Sci. Sports 19 (6) (2009 Dec) 782–789.
[32] V. Di Felice, F. Macaluso, A. Montalbano, A.M. Gammazza, D. Palumbo, T. Angelone, M. Bellafiore, F. Farina, Effects of conjugated linoleic acid and endurance training on peripheral blood and bone marrow of trained mice, J. Strength Cond. Res. 21 (1) (2007 Feb) 193–198.
[33] R. Barone, F. Rappa, F. Macaluso, C. Caruso Bavisotto, C. Sangiorgi, G. Di Paola, G. Tomasello, V. Di Felice, V. Marcianò, F. Farina, G. Zummo, E. Conway de Macario, A.J. Macario, M. Cocchi, F. Cappello, A. Marino Gammazza, Alcoholic liver disease: a mouse model reveals protection by lactobacillus fermentum, Clin. Transl. Gastroenterol. 7 (2016 Jan 21) e138.
[34] R. Barone, F. Macaluso, C. Sangiorgi, C. Campanella, A. Marino Gammazza, V. Moresi, D. Coletti, E. Conway de Macario, A.J. Macario, F. Cappello, S. Adamo, F. Farina, G. Zummo, V. Di Felice, Skeletal muscle Heat shock protein 60 increases after endurance training and induces peroxisome proliferator-activated receptor gamma coactivator 1 α1 expression, Sci. Rep. 6 (2016 Jan 27) 19781.
[35] R. Barone, C. Sangiorgi, A. Marino Gammazza, D. D'Amico, M. Salerno, F. Cappello, C. Pomara, G. Zummo, F. Farina, V. Di Felice, F. Macaluso, Effects of conjugated linoleic acid associated with endurance exercise on muscle fibres and peroxisome proliferator-activated receptor γ coactivator 1 α isoforms, J. Cell. Physiol. 232 (5) (2017 May) 1086–1094.
[36] D.M. Brown, T. Parr, J.M. Brameld, Myosin heavy chain mRNA isoforms are expressed in two distinct cohorts during C2C12 myogenesis, J. Muscle Res. Cell Motil. 32 (6) (2012 Mar) 383–390, https://doi.org/10.1007/s10974-011-9267-4.
[37] A. Weydert, P. Barton, J.A. Harris, C. Pinset, M. Buckingham, Development pattern of mouse myosin heavy chain gene transcripts in vivo and in vitro, Cell 49 (1987) 121–129.
[38] E. Grazioli, I. Dimauro, N. Mercatelli, G. Wang, Y. Pitsiladis, L. Di Luigi, D. Caporossi, Physical activity in the prevention of human diseases: role of epigenetic modifications, BMC Genomics 18 (Suppl 8) (2017 Nov 14) 802, https://doi.org/10.1186/s12864-017-4193-5.
[39] J.A. Hawley, M. Hargreaves, M.J. Joyner, J.R. Zierath, Integrative biology of exercise, Cell 159 (2014) 738–749, https://doi.org/10.1016/j.cell.2014.10.029.
[40] P.D. Neufer, M.M. Bamman, D.M. Muoio, C. Bouchard, D.M. Cooper, B.H. Goodpaster, Booth, et al., Understanding the cellular and molecular mechanisms of physical activity-induced health benefits, Cell Metabol. 22 (1) (2015 Jul 7) 4–11.
[41] K. Azizbeigia, R.S. Stannard, A. Atashakc, M.M. Haghighid, Antioxidant enzymes and oxidative stress adaptation to exercise training: comparison of endurance, resistance, and concurrent training in untrained males, J. Exerc. Sci. Fit. 12 (1) (2014) 1–6 https://doi.org/10.1016/j.jesf.2013.12.001.
[42] M.R. Beltran Valls, I. Dimauro, A. Brunelli, E. Tranchita, E. Ciminelli, P. Caserotti, G. Duranti, S. Sabatini, P. Parisi, A. Parisi, D. Caporossi, Explosive type of moderate-resistance training induces functional, cardiovascular, and molecular adaptations in the elderly, Age (Dordr) 36 (2) (2014 Apr) 759–772, https://doi.org/10.1007/s11357-013-9584-1.
[43] I. Dimauro, M. Scalabrin, C. Fantini, E. Grazioli, M.R. Beltran Valls, N. Mercatelli, A. Parisi, S. Sabatini, L. Di Luigi, D. Caporossi, Resistance training and redox homeostasis: correlation with age-associated genomic changes, Redox Biol. 10 (2016) 34–44, https://doi.org/10.1016/j.redox.2016.09.008.
[44] I. Dimauro, A. Sgura, M. Pittaluga, F. Magi, C. Fantini, R. Mancinelli, A. Sgadari, S. Fulle, D. Caporossi, Regular exercise participation improves genomic stability in diabetic patients: an exploratory study to analyse telomere length and DNA damage, Sci. Rep. 7 (1) (2017 Jun 23) 4137, https://doi.org/10.1038/s41598-017-04448-4.
[45] E. Fehrenbach, F. Passek, A.M. Niess, H. Pohla, C. Weinstock, H.H. Dickhuth, H. Northoff, HSP expression in human leukocytes is modulated by endurance exercise, Med. Sci. Sports Exerc. 32 (3) (2000) 592–600.
[46] M.C. Gomez-Cabrera, E. Domenech, J. Viña, Moderate exercise is an antioxidant: upregulation of antioxidant genes by training, Free Radic. Biol. Med. 44 (2) (2008 Jan 15) 126–131, https://doi.org/10.1016/j.freeradbiomed.2007.02.001.
[47] M. Pittaluga, A. Sgadari, I. Dimauro, B. Tavazzi, P. Parisi, D. Caporossi, Physical exercise and redox balance in type 2 diabetics: effects of moderate training on biomarkers of oxidative stress and DNA damage evaluated through comet assay, Oxid. Med. Cell Longev. 2015 (2015) 981242, https://doi.org/10.1155/2015/981242.
[48] N. Golenhofen, M.D. Perng, R.A. Quinlan, D. Drenckhahn, Comparison of the small heat shock proteins alphaB-crystallin, MKBP, HSP25, HSP20, and cvHSP in heart and skeletal muscle, Histochem. Cell Biol. 122 (2004) 415–425.
[49] R. Bottinelli, S. Schiaffino, C. Reggiani, Force-velocity relations and myosin heavy chain isoform compositions of skinned fibres from rat skeletal muscle, J. Physiol. 437 (1991) 655–672.
[50] S. Schiaffino, C. Reggiani, Fiber types in mammalian skeletal muscles, Physiol. Rev. 91 (4) (2011 Oct) 1447–1531, https://doi.org/10.1152/physrev.00031.2010.
[51] A. McArdle, D. Pattwell, A. Vasilaki, R.D. Griffiths, M.J. Jackson, Contractile activity-induced oxidative stress: cellular origin and adaptive responses, Am. J. Physiol. Cell Physiol. 280 (3) (2001) C621–C627 2001 Mar.
[52] P. Steinbacher, P. Eckl, Impact of oxidative stress on exercising skeletal muscle, Biomolecules 5 (2015) 356–377.
[53] S.K. Powers, M.J. Jackson, Exercise-induced oxidative stress: cellular mechanisms and impact on muscle force production, Physiol. Rev. 88 (4) (2008 Oct) 1243–1276, https://doi.org/10.1152/physrev.00031.2007.
[54] M.R. Beltran Valls, D.J. Wilkinson, M.V. Narici, K. Smith, B.E. Phillips, D. Caporossi, P.J. Atherton, Protein carbonylation and heat shock proteins in human skeletal muscle: relationships to age and sarcopenia, J. Gerontol. A Biol. Sci. Med. Sci. 70 (2) (2015 Feb) 174–181, https://doi.org/10.1093/gerona/glu007.
[55] S. Goto, A. Nakamura, Z. Radak, H. Nakamoto, R. Takahashi, et al., Carbonylated proteins in aging and exercise: immunoblot approaches, Mech. Ageing Dev. 107 (1999) 245–253 S004763749800133X [pii].
[56] E. Niki, Lipid peroxidation products as oxidative stress biomarkers, Biofactors 34 (2) (2008) 171–180.
[57] Z. Radak, T. Kaneko, S. Tahara, H. Nakamoto, H. Ohno, et al., The effect of exercise training on oxidative damage of lipids, proteins, and DNA in rat skeletal muscle: evidence for beneficial outcomes, Free Radic. Biol. Med. 27 (1999) 69–74 S0891-5849(99)00038-6 [pii].
[58] E.R. Stadtman, R.L. Levine, Free radical-mediated oxidation of free amino acids and amino acid residues in proteins, Amino Acids 25 (2003) 207–218, https://doi.org/10.1007/s00726-003-0011-2.
[59] M. Xiao, H. Zhong, L. Xia, Y. Tao, H. Yin, Pathophysiology of mitochondrial lipid oxidation: role of 4-hydroxynonenal (4-HNE) and other bioactive lipids in mitochondria, Free Radic. Biol. Med. 111 (2017 Oct) 316–327, https://doi.org/10.1016/j.freeradbiomed.2017.04.363.
[60] R.A. Pinho, D.M. Sepa-Kishi, G. Bikopoulos, M.V. Wu, A. Uthayakumar, A. Mohasses, M.C. Hughes, C.G.R. Perry, R.B. Ceddia, High-fat diet induces skeletal muscle oxidative stress in a fiber type-dependent manner in rats, Free Radic. Biol. Med. 110 (2017 Sep) 381–389, https://doi.org/10.1016/j.freeradbiomed.2017.07.005.
[61] M. Takahashi, K. Suzuki, H. Matoba, S. Sakamoto, S. Obara, Effects of different intensities of endurance exercise on oxidative stress and antioxidant capacity, J. Phys. Fit. Sports Med. 1 (1) (2012) 183–189.
[62] I. Dimauro, N. Mercatelli, D. Caporossi, Exercise-induced ROS in heat shock proteins response, Free Radic. Biol. Med. 98 (2016) 46–55, https://doi.org/10.1016/j.freeradbiomed.2016.03.028.
[63] Y. Atomi, K. Toro, T. Masuda, H. Hatta, Fiber-type-specific alphaB-crystallin distribution and its shifts with T(3) and PTU treatments in rat hindlimb muscles, J. Appl. Physiol. 88 (4) (1985) 1355–1364 2000 Apr.
[64] M. Haslbeck, S. Weinkauf, J. Buchner, Regulation of the chaperone function of small Hsps, in: L.E. Hightower (Ed.), Tanguay RM, Springer International Publishing, Switzerland, The Small HSP World. Cham, 2015isbn:978-3-319-16076-4.
[65] J. Peschek, N. Braun, J. Rohrberg, et al., Regulated structural transitions unleash the chaperone activity of aB-crystallin, Proc. Natl. Acad. Sci. U. S. A. 110 (E3780e) (2013) E3789.
[66] A.P. Arrigo, Human small heat shock proteins: protein interactomes of homo- and hetero-oligomeric complexes: an update, FEBS Lett. 587 (13) (2013) 1959–1969.
[67] A.P. Arrigo, B. Gibert, Protein interactomes of three stress inducible small heat shock proteins: HspB1, HspB5 and HspB8, Int. J. Hyperth. 29 (5) (2013) 409–422.
[68] A.T. McDuffee, G. Senisterra, S.A. Huntley, J.R. Lepock, K.R. Sekhar, M.J. Meredith, M.J. Borrelli, J.D. Morrow, M.L. Freeman, Proteins containing non-native disulfide bonds generated by oxidative stress can act as signals for the induction of the heat shock response, J. Cell. Physiol. 171 (1997) 143–151.
[69] O. Gonchar, Muscle fiber specific antioxidative system adaptation to swim training

in rats: influence of intermittent hypoxia, J. Sport. Sci. Med. 4 (2) (2005 Jun 1) 160–169.
[70] J. Hollander, R. Fiebig, M. Gore, J. Belma, T. Ookawara, H. Ohno, L.L. Ji, Superoxide dismutase gene expression in skeletal muscle: fiber-specific adaptation to endurance training, Am. J. Physiol. (Regul. Integr. Comp. Physiol.) 277 (1999) R856–R862.
[71] R. Bakthisaran, K.K. Akula, R. Tangirala, ChM. Rao, Phosphorylation of αB-crystallin: role in stress, aging and patho-physiological conditions, Biochim. Biophys. Acta 1860 (2016 Jan) 167–182.
[72] P. Verschuure, Y. Croes, I.P.R. van den, R.A. Quinlan, W.W. de Jong, W.C. Boelens, Translocation of small heat shock proteins to the actin cytoskeleton upon proteasomal inhibition, J. Mol. Cell. Cardiol. 34 (2002) 117–128.
[73] O. Agbulut, P. Noirez, F. Beaumont, G. Butler-Browne, Myosin heavy chain isoforms in postnatal muscle development of mice, Biol. Cell 95 (2003) 399–406.
[74] S. Burattini, P. Ferri, M. Battistelli, R. Curci, F. Luchetti, E. Falcieri, C2C12 murine myoblasts as a model of skeletal muscle development: morpho-functional characterization, Eur. J. Histochem. 48 (2004) 223–233.
[75] J.B. Miller, Myogenic programs of mouse muscle cell lines: expression of myosin heavy chain isoforms, MyoD1, and myogenin, J. Cell Biol. 111 (1990) 1149–1159.
[76] L. Silberstein, S.G. Webster, M. Travis, H.M. Blau, Developmental progression of myosin gene expression in cultured muscle cells, Cell 46 (1986) 1076–1081.
[77] J.M. Peake, J.F. Markworth, K. Nosaka, T. Raastad, G.D. Wadley, V.G. Coffey, Modulating exercise-induced hormesis: does less equal more? J. Appl. Physiol. 119 (3) (1985) 172–189, https://doi.org/10.1152/japplphysiol.01055.2014 2015 Aug 1.
[78] H. Sies, Hydrogen peroxide as a central redox signaling molecule in physiological oxidative stress: oxidative eustress, Redox Biol. 11 (2017) 613–619, https://doi.org/10.1016/j.redox.2016.12.035.
[79] M. Khassaf, R.B. Child, A. McArdle, D.A. Brodie, C. Esanu, M.J. Jackson, Time course of responses of human skeletal muscle to oxidative stress induced by non-damaging exercise, J. Appl. Physiol. 90 (2001) 1031–1035.
[80] H.E. Hoover, D.J. Thuerauf, J.J. Martindale, C.C. Glembotski, Alpha B-crystallin gene induction and phosphorylation by MKK6-activated p38. A potential role for alpha B-crystallin as a target of the p38 branch of the cardiac stress response, J. Biol. Chem. 275 (31) (2000 Aug 4) 23825–23833.
[81] N. Launay, B. Goudeau, K. Kato, P. Vicart, A. Lilienbaum, Cell signaling pathways to alphaB-crystallin following stresses of the cytoskeleton, Exp. Cell Res. 312 (18) (2006 Nov 1) 3570–3584.
[82] E. Shu, H. Matsuno, S. Akamastu, Y. Kanno, H. Suga, K. Nakajima, A. Ishisaki, S. Takai, K. Kato, Y. Kitajima, O. Kozawa, alphaB-crystallin is phosphorylated during myocardial infarction: involvement of platelet-derived growth factor-BB, Arch. Biochem. Biophys. 438 (2) (2005 Jun 15) 111–118.
[83] H. Ito, K. Okamoto, H. Nakayama, T. Isobe, K. Kato, Phosphorylation of alphaB-crystallin in response to various types of stress, J. Biol. Chem. 272 (47) (1997) 29934–29941 https://doi.org/10.1074/jbc.272.47.29934.
[84] K. Kato, H. Ito, K. Kamei, Y. Inaguma, I. Iwamoto, S. Saga, Phosphorylation of alphaB-crystallin in mitotic cells and identification of enzymatic activities responsible for phosphorylation, J. Biol. Chem. 273 (43) (1998 Oct 23) 28346–28354.
[85] I.K. Aggeli, I. Beis, C. Gaitanaki, Oxidative stress and calpain inhibition induce alpha B-crystallin phosphorylation via p38-MAPK and calcium signalling pathways in H9c2 cells, Cell. Signal. 20 (7) (2008 Jul) 1292–1302, https://doi.org/10.1016/j.cellsig.2008.02.019.
[86] C.E. Voorter, W.A. de Haard-Hoekman, E.S. Roersma, H.E. Meyer, H. Bloemendal, W.W. de Jong, The in vivo phosphorylation sites of bovine alpha B-crystallin, FEBS Lett. 259 (1) (1989 Dec 18) 50–52.
[87] A. Shiryaev, G. Dumitriu, U. Moens, Distinct roles of MK2 and MK5 in cAMP/PKA- and stress/p38MAPK-induced heat shock protein 27 phosphorylation, J. Mol. Signal. 6 (1) (2011 May 16) 4, https://doi.org/10.1186/1750-2187-6-4.
[88] T.P. Stossel, J. Condeelis, L. Cooley, J.H. Hartwig, A. Noegel, M. Schleicher, S.S. Shapiro, Filamins as integrators of cell mechanics and signalling, Nat. Rev. Mol. Cell Biol. 2 (2001) 138–145, https://doi.org/10.1038/35052082.
[89] Y. Feng, C.A. Walsh, The many faces of filamin: a versatile molecular scaffold for cell motility and signalling, Nat. Cell Biol. 6 (2004) 1034–1038, https://doi.org/10.1038/ncb1104-1034.
[90] L.Y. Juo, W.C. Liao, Y.L. Shih, B.Y. Yang, A.B. Liu, Y.T. Yan, HSPB7 interacts with dimerized FLNC and its absence results in progressive myopathy in skeletal muscles, J. Cell Sci. 129 (8) (2016 Apr 15) 1661–1670, https://doi.org/10.1242/jcs.179887.
[91] I. Wojtowicz, J. Jablonska, M. Zmojdzian, O. Taghli-Lamallem, Y. Renaud, G. Junion, M. Daczewska, S. Huelsmann, K. Jagla, T. Jagla, Drosophila small heat shock protein CryAB ensures structural integrity of developing muscles, and proper muscle and heart performance, Development 142 (2015) 994–1005.